Accepted Manuscript

Analyzing the function of the insert region found between the α and β-subunits in the eukaryotic nitrile hydratase from *Monosiga brevicollis*

Xinhang Yang, Brian Bennett, Richard C. Holz

PII: S0003-9861(18)30338-2

DOI: 10.1016/j.abb.2018.08.013

Reference: YABBI 7800

To appear in: *Archives of Biochemistry and Biophysics*

Received Date: 27 April 2018

Revised Date: 30 August 2018

Accepted Date: 31 August 2018

Please cite this article as: X. Yang, B. Bennett, R.C. Holz, Analyzing the function of the insert region found between the α and β-subunits in the eukaryotic nitrile hydratase from *Monosiga brevicollis*, *Archives of Biochemistry and Biophysics* (2018), doi: 10.1016/j.abb.2018.08.013.

Analyzing the Function of the Insert Region Found Between the α and β-Subunits in the Eukaryotic Nitrile Hydratase from *Monosiga brevicollis*†

Xinhang Yang,[1] Brian Bennett,[2] and Richard C. Holz[1,*]

[1]*Department of Chemistry, Marquette University, PO Box 1881, Milwaukee, Wisconsin 53201 and the* [2]*Department of Physics, Marquette University, PO Box 1881, Milwaukee, Wisconsin 53201-1881*

†This work was supported by National Science Foundation (CHE-1808711, RCH and BB; CHE-1532168 BB & RCH), the Todd Wehr Foundation, Bruker Biospin, and the National Institutes of Health/NIBIB National Biomedical EPR Center (P41-EB001980).

*To whom correspondence should be addressed: Richard C. Holz, Department of Chemistry, Marquette University, PO Box 1881, Milwaukee, WI 53201, Phone (414) 288-7230, E-mail: richard.holz@marquette.edu

Abstract

The functional roles of the $(His)_{17}$ region and an insert region in the eukaryotic nitrile hydratase (NHase, EC 4.2.1.84) from *Monosiga brevicollis* (*Mb*NHase), were examined. Two deletion mutants, *Mb*NHase$^{\Delta 238\text{-}257}$ and *Mb*NHase$^{\Delta 219\text{-}272}$, were prepared in which the $(His)_{17}$ sequence and the entire insert region were removed. Each of these *Mb*NHase enzymes provided an $\alpha_2\beta_2$ heterotetramer, identical to that observed for prokaryotic NHases and contains their full complement of cobalt ions. Deletion of the $(His)_{17}$ motif provides an *Mb*NHase enzyme that is ~55% as active as the WT enzyme when expressed in the absence of the Co-type activator (ε) protein from *Pseudonocardia thermophila* JCM 3095 (*Pt*NHase^{act}) but ~28% more active when expressed in the presence of *Pt*NHase^{act}. *Mb*NHase$^{\Delta 219\text{-}272}$ exhibits ~55% and ~89% of WT activity, respectively, when expressed in the absence or presence of *Pt*NHase^{act}. Proteolytic cleavage of *Mb*NHase provides an $\alpha_2\beta_2$ heterotetramer that is modestly more active compared to WT *Mb*NHase (k_{cat} = 163 $\pm$ 4 vs 131 $\pm$ 3 s^{-1}). Combination of these data establish that neither the $(His)_{17}$ nor the insert region are required for metallocentre assembly and maturation, suggesting that Co-type eukaryotic NHases utilize a different mechanism for metal ion incorporation and post-translational activation compared to prokaryotic NHases.

Keywords

Nitrile hydratase, enzyme kinetics, cobalt, protein biosynthesis, metal transport, and metal insertion.

Introduction

Nitrile hydratases (NHases, EC 4.2.1.84) are metalloenzymes that contain either a non-heme Fe(III) ion (Fe-type) or a non-corrin Co(III) ion (Co-type) in their active site [1, 2]. NHases catalyze the hydration of nitriles to their corresponding higher value amides under mild conditions (room temperature and physiological pH) and have attracted substantial interest as biocatalysts in preparative organic chemistry and bioremediation processes [3-8]. NHases have historically been only found in prokaryotes; however, multiple eukaryotic organisms were shown to contain genes that potentially encode NHase enzymes [9, 10]. We recently cloned and over-expressed the candidate gene from the eukaryotic organism *Monosiga brevicollis* in *E. coli* and characterized a fully functional Co-type NHase gene product, with fused α- and β-subunits linked by a $(His)_{17}$ containing region (*Mb*NHase) (Figure 1) [11]. Size-exclusion chromatography indicated that *Mb*NHase is an $(\alpha\beta)_2$ homodimer in solution, analogous to the $\alpha_2\beta_2$ heterotetrameric architecture of prokaryotic NHases, of which numerous X-ray crystal structures exist [1, 2, 12, 13].

Several open reading frames (ORFs) have been identified just downstream from the structural α- and β-subunit genes in prokaryotic NHases, and one of these genes has been proposed to function as an activator (*ε*) protein [14-16]. The prevailing dogma is that both Co- and Fe-type NHase enzymes require the co-expression of an (*ε*) protein to be fully metallated, post-translationally modified, and fully functional [14-16]. No such (*ε*) protein has been identified for eukaryotic NHases, such as *Mb*NHase [9, 10]. It is tempting to speculate that the insert region within *Mb*NHase, which contains a $(His)_{17}$ motif, plays the role of the (*ε*) protein. Histidine rich regions are present in some cobalamin (vitamin B12)

biosynthetic pathway proteins, *e.g.*, the chelatase CbiX enzyme from *Bacillus megaterium* and CobW from *Pseudomonas denitrificans* [17]. Histidine rich regions are also found in accessory proteins involved in metallocentre assembly of nickel hydrogenases and ureases, such as HypB from *Bradyrhizobium japonicum* and *Rhizobium leguminosarum*, SlyD from *Escherichia coli* and *Helicobacter pylori*, UreE from *Klebsiella aerogenes*, and Hpn and Hpn-like proteins from *Helicobacter pylori* [18].

To investigate metallocentre assembly in *Mb*NHase, we created three different altered *Mb*NHase enzymes. First, we obtained a proteolytically cleaved *Mb*NHase enzyme in which the α- and β-subunits were separated providing an enzyme that structurally mimics prokaryotic NHase enzymes. Second, a mutant MbNHase enzyme, in which the entire $(His)_{17}$ motif was removed (*Mb*NHase$^{\Delta 238\text{-}257}$), was constructed and expressed in the presence and absence of the prototypical prokaryotic Co-type (ε) activator protein from *Pseudonocardia thermophila* JCM 3095 (*Pt*NHase^{act}). Finally, a mutant was constructed in which the entire insert region was deleted (*Mb*NHase$^{\Delta 219\text{-}272}$), leaving only the classical prokaryotic NHase α- and β-subunit analogs; this mutant was also expressed in the presence and absence *Pt*NHase^{act}. Functional interrogation of these species provides important insight into the role of the insert region in *Mb*NHase and how eukaryotic NHase enzymes are metallated and post-translationally modified.

Materials and Methods

Materials. Acrylonitrile, 2-Amino-2-hydroxymethyl-propane-1,3-diol (Tris-HCl),

and 4-(2-hydroxyethyl)piperazine-1-ethanesulfonic acid (HEPES) were obtained from Sigma-Aldrich. Oligonucleotides and genes were obtained from Integrated DNA Technologies, Inc. All other reagents were purchased commercially and were the highest purity available.

Expression and Purification of MbNHase. Protein sequences for the α- and β-subunit genes of the putative WT *Mb*NHase were obtained from ORF 37534 (UniProt ID A9V2C1.1) of *M. brevicollis* and the predicted gene was synthesized by Integrated DNA Technologies, Inc. with optimized *E. coli* codon usage. This gene was cloned into the kanamycin resistant pET21a$^+$ (EMD Biosciences) expression vector to create the plasmid pSMMαβ, as previously reported [11].

A single colony was used to inoculate separate starter cultures of 50 mL LB Miller media containing the appropriate antibiotics (pET28a+: 50 mg/mL kanamycin) and allowed to grow at 37 °C with constant shaking overnight. These cultures were used to inoculate 6 L of LB Miller media containing the appropriate antibiotics and allowed to grow at 37 °C with constant shaking until an optical density of ~0.8-1.0 at 600 nm was reached. The cultures were cooled on ice to 20 °C and induced with 0.1 mM Isopropyl-β-D-1-thiogalactopyranoside (IPTG), supplemented with 0.25 mM of $CoCl_2$, and shaken for an additional 16 hours at 20 °C.

Cells were pelleted by centrifugation at 6,370 × *g* for 10 minutes at 4 °C in a Beckman Coulter Avanti JA-10 rotor and resuspended in buffer **A** (50 mM sodium phosphate buffer, pH 7.5, containing 300 mM NaCl, 5% glycerol, and 10 mM imidazole) at a ratio of 5 mL per gram of cells. Cells were lysed by ultrasonication (Misonix Sonicator 3000) for 4

min (alternating 30s on and 45s off) at 21 W. Cell lysate was separated from cell debris by centrifugation in a JA-20 rotor at 31,000 × *g* at 4 °C for 20 min. Cell lysate was purified using immobilized metal affinity chromatography (IMAC; 100 mg protein/5mL column) on a GE ÄKTA Fast Protein Liquid Chromatography (FPLC) system at 4 °C. The column was washed with 50 mL of buffer **A** followed by 50 mL of buffer **A** containing additional imidazole (35 mM). The protein was eluted using a linear gradient (0-100%) of buffer **B** (50 mM NaH_2PO_4 pH 7.5, 300 mM NaCl, 10% glycerol, 525 mM imidazole) at a flow rate of 1 mL/min resulting in *Mb*NHase being eluted between 150 to 240 mM imidazole.

Fractions containing WT *Mb*NHase were pooled and concentrated to ~1 mL using an Amicon Ultra-15 (Millipore) and loaded onto a 16/60 Superdex 200 prep grade (GE Healthcare) polishing column using buffer **C** (50 mM HEPES and 300 mM NaCl at pH 8.0). Pure WT *Mb*NHase was concentrated using an Amicon Ultra-15 (Millipore) and analyzed by SDS-PAGE with a 12.5% polyacrylamide SPRINT NEXT GEL™ (Amresco). Gels were stained with Gel Code Blue (Thermo-Fisher Scientific). The protein concentration of purified WT *Mb*NHase was determined by measuring the absorbance at 280 nm on a Shimadzu UV-2450 spectrophotometer. The calculated molecular weight for the WT *Mb*NHase homodimer is 111,207 g/mol with an extinction coefficient of 143,700 cm^{-1} M^{-1}. The molecular weight is in good agreement with SDS-PAGE data [11].

Expression and Purification of MbNHase Mutants. The genes encoding for the *Mb*NHase α- and β-subunits, where the entire $(His)_{17}$ motif was removed (*Mb*NHase$^{\Delta 238\text{-}257}$), were synthesized by Integrated DNA Technologies, Inc. with optimized *E. coli* codon usage and cloned into the kanamycin resistant pET28a$^+$ (EMD Biosciences) plasmid. The α- and

β-subunit genes were designed for co-expression by overlapping the "TGA" stop codon of the β-subunit with the "ATG" start codon of the α subunit (Figure SI-1), like the expression of *Pt*NHase [16]. In addition, the α- and β-subunit genes where the entire insert region was deleted (*Mb*NHase$^{\Delta 219\text{-}272}$), were obtained by polymerase chain reaction (PCR) using the primers (Sense primer: CAACCATGGGTACCG AGCAGGCGGCGGTG; Anti-sense primer: CATAAGCTTTTAGTGGTGGTGGTGATGATGATCAACACGCGGCA) for the α-subunit and (Sense primer: ACG CATATG ATGCACCTGT TCA CCTACGACCTGCA; Anti-sense primer: AGTCCTCGAGTTACGCTTG CGGCGGGTTGCTA) for the β-subunit. The α-subunit gene was sub-cloned between *NcoI* and *HindIII* sites, while the β-subunit gene was sub-cloned between *NdeI* and *XhoI* sites within the pCOLADuet-1 expression vector (Novagen). The sequences were confirmed by Functional Biosciences. The plasmids containing the *Mb*NHase$^{\Delta 238\text{-}257}$ and *Mb*NHase$^{\Delta 219\text{-}272}$ deletion mutant genes were transformed into BL21 magic cells for the soluble expression of the *Mb*NHase$^{\Delta 238\text{-}257}$ and *Mb*NHase$^{\Delta 219\text{-}272}$ enzymes. Expression and purification of these mutant enzymes were carried out in an identical manner to that described above for WT *Mb*NHase [11].

Expression and Purification of WT MbNHase and the Mutants in the Absence or Presence of PtNHase^{act}. The gene encoding the Co-type activator (ε) protein from *Pseudonocardia thermophila* JCM 3095 (*Pt*NHase^{act}) was synthesized by Integrated DNA Technologies, Inc. with optimized *E. coli* codon usage and cloned into the kanamycin resistant pET21a^{+} (EMD Biosciences) expression vector to create the pSPT^{act} plasmid. The pSPT^{act} plasmid was co-expressed with the previously reported pSMMαβ plasmid encoding recombinant *MbNHase* [11] that had been freshly transformed into BL21(DE3) (Stratagene)

competent cells. In addition, the pSPT^{act} plasmid was co-expressed with the plasmids containing the *Mb*NHase$^{\Delta 238\text{-}257}$ and *Mb*NHase$^{\Delta 219\text{-}272}$ deletion mutant genes in BL21 magic cells. Expression and purification of WT *Mb*NHase, *Mb*NHase$^{\Delta 238\text{-}257}$ and *Mb*NHase$^{\Delta 219\text{-}272}$ co-expressed with *Pt*NHase^{act} was carried out in an identical manner to that described above for WT *Mb*NHase [11].

Kinetic Analysis. The enzymatic activity of WT *Mb*NHase and each variant was determined using acrylonitrile as the substrate (acrylamide; $\Delta\varepsilon_{225} = 2.9\ mM^{-1}\ cm^{-1}$). The rate of nitrile hydration was determined by continuously monitoring the formation of acrylamide at 225 nm using a Shimadzu UV-2450 spectrophotometer equipped with a TCC-240A temperature controlled cell holder [19]. A typical 1 mL reaction consisted of 50 mM Tris-HCl buffer pH 7.0 at 25 °C and various concentrations of acrylonitrile (0 to 450 mM). One unit (U) of *Mb*NHase activity is defined as the formation of 1 µmol of acrylamide per minute. To obtain the kinetic parameters, V_{max} and K_m, the initial velocities from at least three independent measurements were fitted to the Michaelis-Menten equation using OriginPro 9.0 (OriginLab, Northampton, MA). Kinetic data for each *Mb*NHase variant was determined more than three times for multiple purifications, all of which provided consistent results.

Metal Analysis. The metal content of WT *Mb*NHase and each variant, expressed in the presence and absence of $CoCl_2$, was determined by inductively-coupled plasma mass spectrometry (ICP-MS). For comparison purposes, the Co-type NHase from *Pseudonocardia thermophila* JCM 3095 (*Pt*NHase) was expressed and purified as previously described [20], and the metal content determined along with a buffer control that contained

no protein. All protein samples were pretreated with 1 M urea and digested with concentrated nitric acid (0.863 mL) followed by heating at 70 °C for 1 h, allowed to cool to room temperature, and then diluted to a final concentration of 5% nitric acid. Samples were submitted for analysis at the Water Quality Center in the College of Engineering at Marquette University (Milwaukee, WI, USA).

Electronic Absorption and Electron Paramagnetic Resonance Spectra. Electronic absorption spectra were recorded on a Shimadzu UV-2450 spectrophotometer equipped with a TCC-240A temperature-controlled cell holder. Spectra for WT *Mb*NHase and each variant as well as *Pt*NHase were obtained at 25 °C in a 1 cm quartz cuvette in 50 mM HEPES buffer containing 300 mM NaCl, pH 8.0. X-band EPR spectra for WT *Mb*NHase were recorded at 4 K, 0.1 mW in 50 mM HEPES buffer containing 300 mM NaCl, pH 8.0 on a Bruker EMXplus spectrometer equipped with an ER4116DM (~ 9.6 GHz) resonator, an Oxford Instruments ESR900 helium flow cryostat, and Oxford Instruments ITC503 temperature controller.

Results and Discussion

Proteolytic Cleavage of WT MbNHase. Active, mature *Mb*NHase was obtained when expressed in the absence of an (ε) protein or the *E. coli* GroES/EL molecular chaperones [11][13], whereas prokaryotic NHase activation appears to absolutely require an activator protein [14-16]. These findings beg the question: “how is *Mb*NHase functionally expressed?” We hypothesized that the insert region, which contains a His_{17} section, (Figure

1) plays a key role in metallocentre assembly and therefore, created three altered *Mb*NHase enzymes targeting this insert region.

Purified WT *Mb*NHase exhibits a single band at ~55 kDa on SDS-PAGE (Figure 2) and a k_{cat} value of 131 ± 3 s^{-1} (K_m = 83 ± 10 mM) in 50 mM Tris-HCl buffer pH 7.0 at 25 °C using acrylonitrile as the substrate, values that are indistinguishable from those reported previously (Table 1) [11]. Size-exclusion chromatography revealed that WT *Mb*NHase exists primarily as an $(\alpha\beta)_2$ homodimer in solution, analogous to the $\alpha_2\beta_2$ heterotetramer architecture observed for prokaryotic NHases. However, storage of WT *Mb*NHase at 4 ℃ in 50 mM Tris-HCl buffer, pH 7.0 for approximately two weeks, provided an *Mb*NHase enzyme with a modestly increased k_{cat} value of 163 ± 4 s^{-1} but a similar K_m value of 93 ± 15 mM, using acrylonitrile as the substrate (Table 1). SDS-PAGE analysis of aged *Mb*NHase samples revealed two polypeptides of ~24 and ~26 kDa (Figure 2), while size exclusion chromatography suggested an $\alpha_2\beta_2$ heterotetramer, identical to that observed for prokaryotic NHases. These data suggested that WT *Mb*NHase is cleaved, likely by trace amounts of proteases. The observed increase in k_{cat} for the proteolytically cleaved *Mb*NHase enzyme, represents an ~20% increase in rate over WT *Mb*NHase. The increased rate was very reproducible for batch-to-batch preparations, providing the calculated error of ± 4 s^{-1}. The observed increase in activity is perhaps due to an easing of conformational stress induced by the insert region in and around the active site, although structural characterization will be required to confirm this.

Confirmation of an $\alpha_2\beta_2$ heterotetramer after proteolytic cleavage of WT *Mb*NHase was obtained by MALDI-TOF mass spectroscopy (Figure 3). Two masses were clearly

observed at 24,848 Da and 25,530 Da, values that are consistent with SDS-PAGE estimates (Figure 2) and correspond to the α- and β-subunits of *Mb*NHase based on sequence comparison with the prototypical Co-type *Pt*NHase enzyme (Figure 4). The two MALDI-TOF MS peaks were of similar intensities, indicating a ~1:1 α:β ratio. Interestingly, the observed molecular masses from MALDI-TOF MS suggests that a 5,226 Da peptide is lost after proteolytic cleavage, comparable to the size of the complete insert region of WT *Mb*NHase. Attempts to isolate the cleaved fragment by gel-filtration were unsuccessful suggesting that the fragment is likely cleaved into small peptides by protease contaminants. Cleavage of *Mb*NHase could be prevented by an additional gel-filtration purification step performed directly after IMAC; however, the addition of metal ion inhibitors such as EDTA or 1,10-phenanthroline had no effect on *Mb*NHase cleavage. Addition of protease inhibitor cocktails, such as AEBSF, resulted in precipitation of *Mb*NHase. Taken together, these data indicate that the single polypeptide of freshly isolated WT *Mb*NHase, which contains fused α- and β-subunits linked by an insert region, is cleaved into separate α- and β-subunits upon ageing, likely by trace amounts of proteases, resulting in a modestly more active $\alpha_2\beta_2$ heterotetrameric form of *Mb*NHase.

A combination of UV-Vis and EPR spectroscopy coupled with metal analyses was used to determine that the proteolytically cleaved *Mb*NHase enzyme contained its full complement of Co(III). ICP-MS data indicated that the proteolytically cleaved *Mb*NHase enzyme contained 1.9 ± 0.1 equivalents of cobalt per $\alpha_2\beta_2$ heterotetramer, indistinguishable from WT *Mb*NHase (Table 1) with no other metal ions detected above the background level of <10 ppb [11]. Proteolytically cleaved *Mb*NHase exhibited the typical amber color of

Co-type NHase enzymes in 50 mM HEPES buffer containing 300 mM NaCl, pH 8.0 (Figure 5) [1], and the UV-Vis spectrum reveals the characteristic S → Co(III) ligand-to-metal-charge-transfer (LMCT) band at 315 nm (ε = 2,500 M^{-1} cm^{-1}) (Figure 5), which is blue-shifted by ~10 nm compared to WT *Mb*NHase [11]. EPR spectra show no detectable Co(II) signals consistent with the presence of low-spin Co(III), which is diamagnetic (Figure SI-2). These data indicate that proteolytically cleaved *Mb*NHase, retains its full complement of Co(III) and that neither the insert region nor the $(His)_{17}$ motif is required for catalysis in the proteolytically cleaved *Mb*NHase enzyme.

Examination of the functional role of the $(His)_{17}$ insert. To investigate whether the $(His)_{17}$ region plays a role in metal ion insertion and/or the posttranslational modification of the active site, the *Mb*NHase$^{\Delta 238\text{-}257}$ $(His)_{17}$ deletion mutant, was prepared. SDS-PAGE analysis revealed two bands at ~25.5 and ~28.5 KDa for *Mb*NHase$^{\Delta 238\text{-}257}$ while size-exclusion chromatography indicated that *Mb*NHase$^{\Delta 238\text{-}257}$ exists primarily as an $\alpha_2\beta_2$ heterotetramer with a molecular weight of ~108 kDa, much like prokaryotic Co-type NHases (Figure 6). Kinetic analyses of the *Mb*NHase$^{\Delta 238\text{-}257}$ $(His)_{17}$ deletion mutant, expressed in the absence or presence of the prototypical Co-type activator (ε) protein, *Pt*NHase^{act}, using acrylonitrile as the substrate, were performed in triplicate for multiple purifications in 50 mM Tris-HCl buffer, pH 7.0 at 25 °C providing k_{cat} values of 71 ± 4 s^{-1} and 166 ± 5 s^{-1} respectively. K_m values for the *Mb*NHase$^{\Delta 238\text{-}257}$ $(His)_{17}$ deletion mutant expressed in the absence or presence of the *Pt*NHase^{act} were 104 ± 17 mM and 125 ± 17 mM, respectively (Table 1). The *Mb*NHase$^{\Delta 238\text{-}257}$ $(His)_{17}$ deletion mutant expressed in the absence or presence of *Pt*NHase^{act} contained 1.8 ± 0.1 and 2.3 ± 0.2 equivalents of cobalt per $\alpha_2\beta_2$

heterotetramer, respectively, with no other metal ions detected above the background level of <10 ppb. The *Mb*NHase$^{\Delta 238\text{-}257}$ $(His)_{17}$ deletion mutant expressed in either the absence or presence of *Pt*NHase^{act} in 50 mM HEPES buffer containing 300 mM NaCl, pH 8.0 exhibited the characteristic S → Co(III) LMCT band at ~320 nm (ε =2,200 M^{-1} cm^{-1}) (Figure 5), nearly identical to WT *Mb*NHase [11]. While the $(His)_{17}$ region is not required for metal uptake or active site maturation, expression in the presence of the prototypical prokaryotic activator protein, *Pt*NHase^{act}, does enhance the observed k_{cat} value by ~60%, which is greater than would be expected from the slight increase (~20%) in metal content. Therefore, *Pt*NHase^{act} does assist in the activation of the *Mb*NHase$^{\Delta 238\text{-}257}$ $(His)_{17}$ deletion mutant but is not required for post-translational modification of the active enzyme.

Investigation of the Insert region of MbNHase. The *Mb*NHase$^{\Delta 219\text{-}272}$ insert region deletion mutation provides an enzyme with the entire insert region between the α and β regions of WT *Mb*NHase removed (Figure 1). Removal of this insert region essentially converts the eukaryotic *Mb*NHase into a prokaryotic NHase analog, allowing the direct comparison of *Mb*NHase$^{\Delta 219\text{-}272}$ and *Pt*NHase. The *Mb*NHase$^{\Delta 219\text{-}272}$ insert region deletion mutant expressed in the absence of *Pt*NHase^{act} exhibited two bands on SDS-PAGE at ~25.5 and ~26.5 kDa. Size-exclusion chromatography indicated that *Mb*NHase$^{\Delta 219\text{-}272}$ exists primarily as an $\alpha_2\beta_2$ heterotetramer with a molecular weight of ~104 kDa, indistinguishable from proteolytically cleaved WT *Mb*NHase and prokaryotic Co-type NHases such as *Pt*NHase. Surprisingly, co-expression of *Mb*NHase$^{\Delta 219\text{-}272}$ in the presence of *Pt*NHase^{act} yielded a single band at ~52 kDa on SDS-PAGE which is consistent with an αβ complex. However, it could also be due to the formation of an $\alpha(\varepsilon)_2$ complex as *Pt*NHase^{act} is ~14 kDa

so an $\alpha(\varepsilon)_2$ complex would have a mass of ~53.5 kDa. Interestingly, the Co-type (ε) protein from *Rhodococcus rhodochrous* J1 was shown to form an $\alpha(\varepsilon)_2$ complex, which was proposed to bind Co(II) and insert it into apo-$\alpha_2\beta_2$ NHase *via* a "self-subunit swapping" mechanism [21]. The Co-type (ε) protein was also proposed to facilitate oxidation of two active site Cys-residues. Attempts to separate the ~52 kDa proteins into their individual components were unsuccessful even in the presence of 8 M urea, 1 M dichlorodiphenyltrichloroethane (DDT) or SDS at 95 °C for 10 min (Figure 7).

Kinetic analysis of the *Mb*NHase$^{\Delta 219\text{-}272}$ insert region deletion mutant expressed in the absence or presence of *Pt*NHase^{act} in 50 mM Tris-HCl buffer, pH 7.0 at 25 °C provided k_{cat} values of 75 ± 8 s^{-1} and 117 ± 10 s^{-1}, respectively, using acrylonitrile as the substrate (Table 1). These kinetic data suggest that the *Mb*NHase$^{\Delta 219\text{-}272}$ insert region deletion mutant expressed in the presence of *Pt*NHase^{act}, is likely an αβ complex, even so, the Co-type NHase (ε) proteins are known to have significant sequence identity with the NHase β-subunit [22, 23], so $\alpha(\varepsilon)_2$ complex might be expected to be catalytically competent, but not likely more active than an $\alpha_2\beta_2$ heterotetramer such as was observed for the *Mb*NHase$^{\Delta 219\text{-}272}$ insert region deletion mutant expressed in the absence of *Pt*NHase^{act}. The *Mb*NHase$^{\Delta 219\text{-}272}$ insert region deletion mutant expressed in the absence or presence of *Pt*NHase^{act} is not particularly stable in 50 mM Tris-HCl buffer, pH 7.0 at 25 °C and loses > 95% of its activity over the course of a few hours, indicating that the insert region plays a role in stabilizing the WT *Mb*NHase enzyme. The *Mb*NHase$^{\Delta 219\text{-}272}$ insert region deletion mutant contained 1.7 ± 0.1 equivalents of cobalt per $\alpha_2\beta_2$ heterotetramer, irrespective of the co-expression of *Pt*NHase^{act}, a value nearly identical to that observed for WT *Mb*NHase (Table 1). UV-Vis spectra of the

*Mb*NHase$^{\Delta 219\text{-}272}$ insert region deletion mutant expressed in the absence or presence of *Pt*NHase^{act} in 50 mM HEPES buffer containing 300 mM NaCl, pH 8.0 were indistinguishable from each other and WT *Mb*NHase (Figure 5). Therefore, *Mb*NHase$^{\Delta 238\text{-}257}$ binds its full complement of Co(III) ions without the assistance of an (ε) protein, indicating that the insert region is also not required for metal ion binding or active site maturation.

Conclusion

Characterization of the eukaryotic NHase from *Monosiga brevicollis* constructs described herein, confirm that *Mb*NHase does not require an NHase activator protein or the *E. coli* chaperone proteins GroEL/ES for metallocentre assembly, including metal ion insertion and active site post-translational maturation. In addition, these data indicate that the $(His)_{17}$ region found within the insert that links the α- and β-subunits is not required for metal ion incorporation or active site maturation. The fact that the proteolytically cleaved WT *Mb*NHase enzyme and the *Mb*NHase$^{\Delta 238\text{-}257}$ $(His)_{17}$ deletion mutant each exhibit a modest increase in activity compared to WT *Mb*NHase, suggests that the insert region likely induces a structural strain on the active site that has a limiting effect on the catalytic rate of hydration. The lack of the need for either an intrinsic or an extrinsic activator polypeptide for *Mb*NHase is in stark contrast to the absolute requirement for an activator for assembly and activation of the otherwise similar prokaryotic NHases. The pertinent and related outstanding questions are, "How can the *Mb*NHase metallocentre self-assemble and self-activate?" and, "Why do the prokaryotic NHase metallocenters require activators for assembly and activation?" The

genetically engineered functional constructs of *Mb*NHase described herein represent an important new tool with which to further address these important questions using structural and spectroscopic methods.

Supporting Information. Supplementary information includes the gene design for the *Mb*NHase$^{\Delta 238\text{-}257}$ mutant (Figure SI-1) and an EPR spectrum of WT *Mb*NHase (Figure SI-2).

Abbreviations. NHase, nitrile hydratase; ORF, open reading frame; ICP-MS, inductively-coupled plasma mass spectrometry; IMAC, immobilized metal affinity chromatography;

References

1 J. A. Kovacs (2004) Chem Rev 104:825-848

2 T. C. Harrop and P. K. Mascharak (2004) Acc Chem Res 37:253-260

3 M. Kobayashi, T. Nagasawa and H. Yamada (1992) Trends Biotechnol 10:402–408

4 T. Nagasawa, H. Shimizu and H. Yamada (1993) Appl Microbiol Biotechnol 40

5 T. Nagasawa and H. Yamada (1995) Pure Appl Chem 67:1241–1256

6 H. Yamada and M. Kobayashi (1996) Biosci Biotech Biochem 60:1391-1400

7 S. Prasad and T. C. Bhalla (2010) Biotechnology Advances 28:725-741

8 T. Nagasawa, C. D. Mathew, J. Mauger and H. Yamada (1988) Appl Environ Microbiol 54:1766-1760

9 A. O. Marron, M. Akam and G. Walker (2012) PLoS ONE 7:e32867

10 K. U. Foerstner, T. Doerks, J. Muller, J. Raes and P. Bork (2008) PLoS ONE 3:e3976

11 S. Martinez, X. Yang, B. Bennett and R. C. Holz (2017) Biochimica et Biophysica Acta (BBA) - Proteins and Proteomics 1865:107-112

12 M. Tsujimura, M. Odaka, H. Nakayama, N. Dohmae, H. Koshino, T. Asami, M. Hoshino, K. Takio, S. Yoshida, M. Maeda and I. Endo (2003) J Am Chem Soc 125:11532-11538

13 A. Dey, M. Chow, K. Taniguchi, P. Lugo-Mas, S. Davin, M. Maeda, J. A. Kovacs, M. Odaka, K. O. Hodgson, B. Hedman and E. I. Solomon (2006) J Am Chem Soc 128:533 - 541

14 M. Nishiyama, S. Horinouchi, M. Kobayashi, T. Nagasawa, H. Yamada and T. Beppu (1991) J Bacteriol 173:2465-2472

15 N. Hashimoto Y., M., Horinouchi S., Beppu T. (1994) Bioscience, biotechnology, and biochemistry 58:1859-1869

16 M. Nojiri, M. Yohda, M. Odaka, Y. Matsushita, M. Tsujimura, T. Yoshida, N. Dohmae, K. Takio and I. Endo (1999) Journal of Biochemistry 125:696-704

17 R. R. Mendel, A. G. Smith, A. Marquet and M. J. Warren (2007) Natural Product Reports 24:963-971

18 K. A. Higgins, C. E. Carr and M. J. Maroney (2012) Biochemistry 51:7816-7832

19 J. M. Stevens, N. Rao Saroja, M. Jaouen, M. Belghazi, J.-M. Schmitter, D. Mansuy, I. Artaud and M.-A. Sari (2003) Protein Expression and Purification 29:70-76

20 S. Martinez, R. Wu, R. Sanishvili, D. Liu and R. Holz (2014) Journal of the American Chemical Society 136:1186-1189

21 Z. Zhou, Y. Hashimoto, T. Cui, Y. Washizawa, H. Mino and M. Kobayashi (2010) Biochemistry 49:9638-9648

22 Z. Zhou, Y. Hashimoto and M. Kobayashi (2009) The Journal of Biological Chemistry 284:14930-14938

23 Z. Zhou, Y. Hashimoto, K. Shiraki and M. Kobayashi (2008) Proceedings of the National Academy of Sciences 105:14849-14854

Table 1. Kinetic constants for the wild-type and mutant *Mb*NHases[a]

	k_{cat} (s^{-1})	K_m (mM)	k_{cat}/K_m ($s^{-1}mM^{-1}$)	Metal Content
Wild-type[b]	131 ± 3	83 ± 10	1.6	1.8 ± 0.1
Cleaved	163 ± 4	93 ± 15	1.8	1.9 ± 0.1
Δ238-257	71 ± 4	104 ± 17	0.7	1.8 ± 0.1
Δ238-257 + *Pt*NHase^{act}	166 ± 5	125 ± 17	1.3	2.3 ± 0.2
Δ219-272	75 ± 8	73 ± 14	1.0	1.7 ± 0.1
Δ219-272 + *Pt*NHase^{act}	117 ± 10	149 ± 23	0.8	1.7 ± 0.1

[a]Acrylonitrile was used as the substrate. [b]Reference [11].

FIGURE CAPTIONS

Figure 1. Scheme showing the arrangement of the NHase β- and α-subunits in eukaryotes.

Figure 2. The SDS-PAGE of (a) WT *Mb*NHase and (b) the proteolytically cleaved *Mb*NHase enzyme.

Figure 3. MALDI-TOF Mass Spectra of proteolytically cleaved *Mb*NHase revealing two peaks at 24.8 and 25.5 kDa corresponding to independent α- and β-subunits.

Figure 4. Sequence alignment of *Mb*NHase and *Pt*NHase shows that the α-subunits share 23% identity while the β-subunits exhibit 32% identity (Orange: active site; green: insert region; yellow: histidine rich region).

Figure 5. UV-Vis spectra of various *Mb*NHase constructs between (a)280 and 500 nm; (b) 300 and 480 nm in 50 mM HEPES buffer containing 300 mM NaCl at pH 8.0. (b)

Figure 6. Purification of the *Mb*NHase$^{\Delta 238\text{-}268}$ mutant. a) size-exclusion column indicating a single peak corresponding to an $\alpha_2\beta_2$ heterotetramer; b) SDS-PAGE gel page showing that the purified α and β-subunits are two independent proteins.

Figure 7. SDS-PAGE gel of *Mb*NHase$^{\Delta 219\text{-}272}$. Column 1: *Mb*NHase$^{\Delta 219\text{-}272}$ from activator co-expression; Column 2: *Mb*NHase$^{\Delta 219\text{-}272}$ from *Pt*NHase activator co-expression treated by 8mM Urea; Column 3: *Mb*NHase$^{\Delta 219\text{-}272}$ from activator co-expression treated by 8M urea and 1M DDT; Column 4: *Mb*NHase$^{\Delta 219\text{-}272}$ without activator.

Figure 1

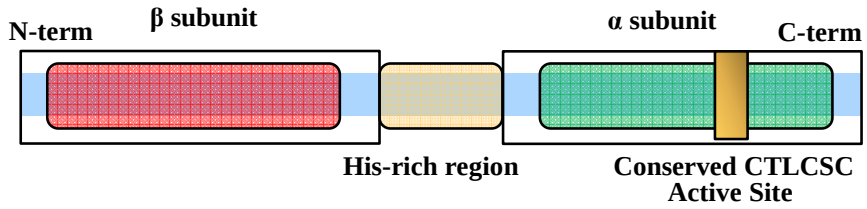

Figure 2

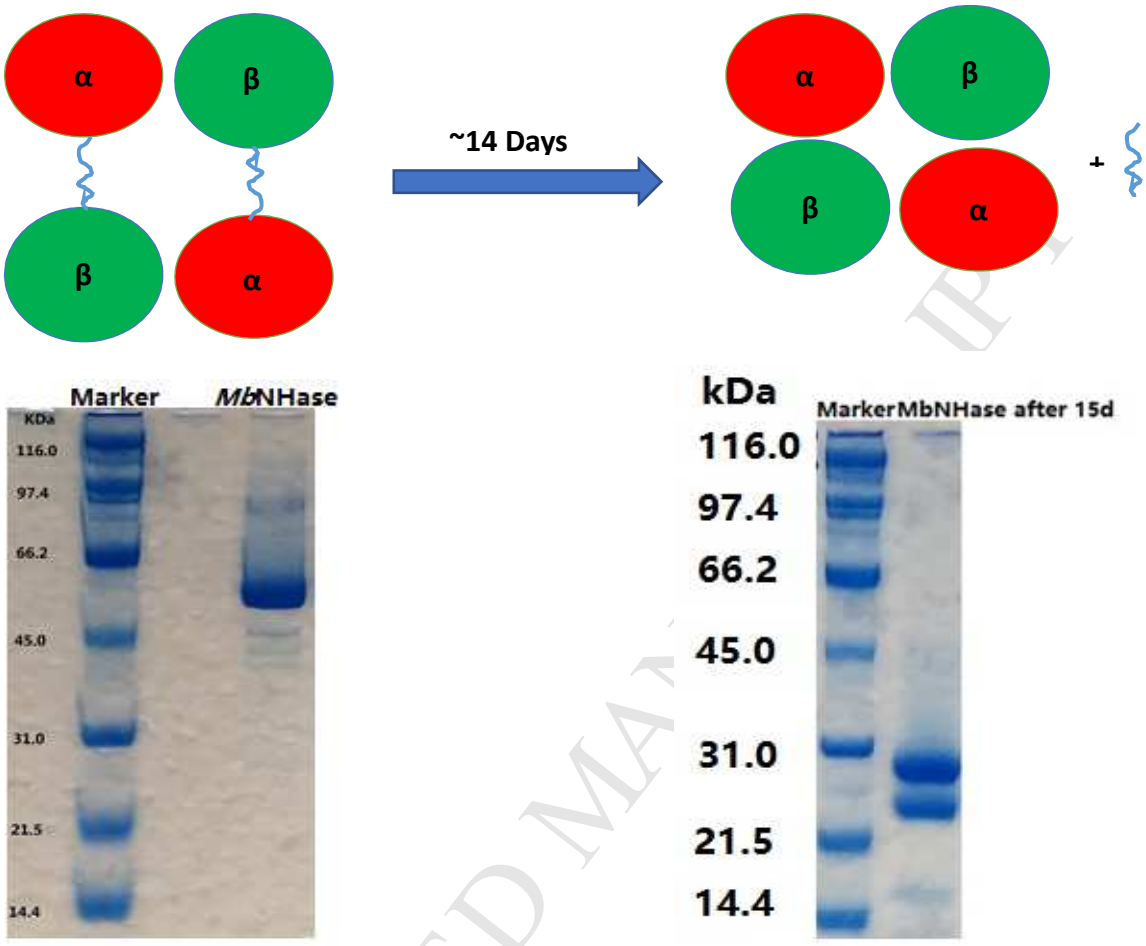

Figure 3

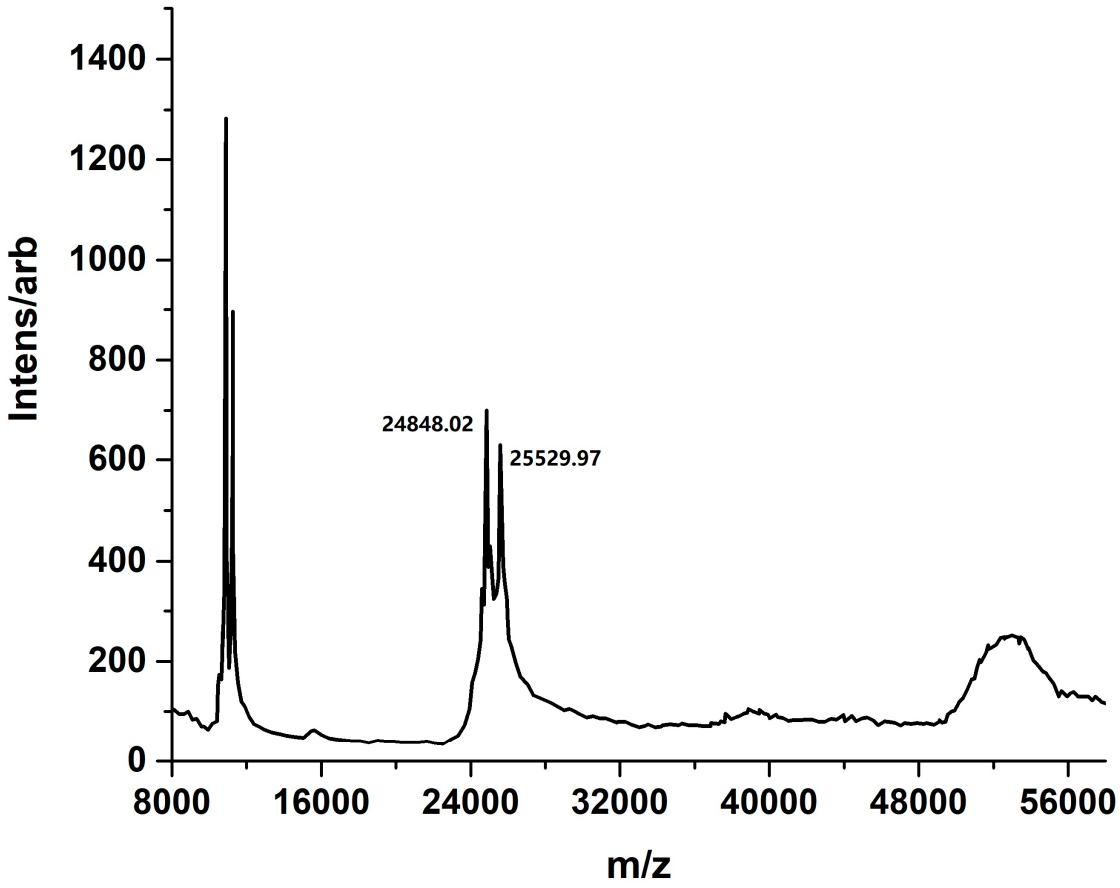

Figure 4


A9V2C1 MbNHase 1 MHLFTYDLHHDVGGAENMLRLPLDRHE-RDYLPWERHIHALVVLLVKQGRMSVDELRRGV 59
Q7SID3 PtNHase β 1 -----MNGVYDVGGTDGLGPINRPADEPVFRAEWEKVAFAMFPATFRAGFMGLDEFRFGI 55
Q7SID2 PtNHase α 1 -- 0
A9V2C1 MbNHase 60 EGLPSSLAEQASYYEKWGLSVSRILTEKGTVSGHELEQG---------- 98
Q7SID3 PtNHase β 56 EQMNPAEYLESPYYWHWIRTYIHHGVRTGKIDLEELERRTQYYRENPDAPLPEHEQKPEL 115
Q7SID2 PtNHase α 1 -- 0
A9V2C1 MbNHase 99 --------FLGVPT-TDLPQVPRFQVGQRVMVRPFGTTFAYRQPHLRVPGYVHGAVGTIV 149
Q7SID3 PtNHase β 116 IEFVNQAVYGGLPASREVDRPPKFKEGDVVRF-----STASPKGHARRARYVRGKTGTVV 170
Q7SID2 PtNHase α 1 -- 0
A9V2C1 MbNHase 150 ELPGLFQDPMTGAYGERGTAQPLYRVAFSHRALWPEGAAHAEPGELEDGVVVDVSQPWLE 209
Q7SID3 PtNHase β 171 KHHGAYIYPDTAGNGLGECPEHLYTVRFTAQELWGPEG------DPNSSVYYDCWEPYIE 224
Q7SID2 PtNHase α 1 -- 0
A9V2C1 MbNHase 210 ALSEADYAQRLATLHRVAFTPDSNPPQA 269
Q7SID3 PtNHase β 225 LVDTKAAAA---------- 233
Q7SID2 PtNHase α 1 -- 0
A9V2C1 MbNHase 270 TRYGTEQAAVAKEAALDFPYQPWCEALVQTLTRRGVVRSDELHATLASLDALQNSGAGPQ 329
Q7SID3 PtNHase β 234 -- 233
Q7SID2 PtNHase α 1 ---MTENILRKSDEEIQKEITARVKALESMLIEQGILTTSMIDRMAEIYENEVGPHLGAK 57
A9V2C1 MbNHase 330 LVARAWSDAAFAEWLLTDAAAAAESLAIRTTNYDADPASAERVGGHRLFSHNHTELRVVA 389
Q7SID3 PtNHase β 234 -- 233
Q7SID2 PtNHase α 58 VVVKAWTDPEFKKRLLADGTEACKELGIGGL----------QGEDMMWVE 97
A9V2C1 MbNHase 390 NTDTVHNLVQ 449
Q7SID3 PtNHase β 234 ---------- 233
Q7SID2 PtNHase α 98 NTDEVHHVVV 157
A9V2C1 MbNHase 450 RVHDSTADLRYMVLPQRPQGTEGWSEEHLRTIVTRDSLLGTAVPRVD 496
Q7SID3 PtNHase β 234 ---------- 233
Q7SID2 PtNHase α 158 KVWDSSSEMRFVVLPQRPAGTDGWSEEELATLVTRESMIGVEPAKAV 204

Figure 5

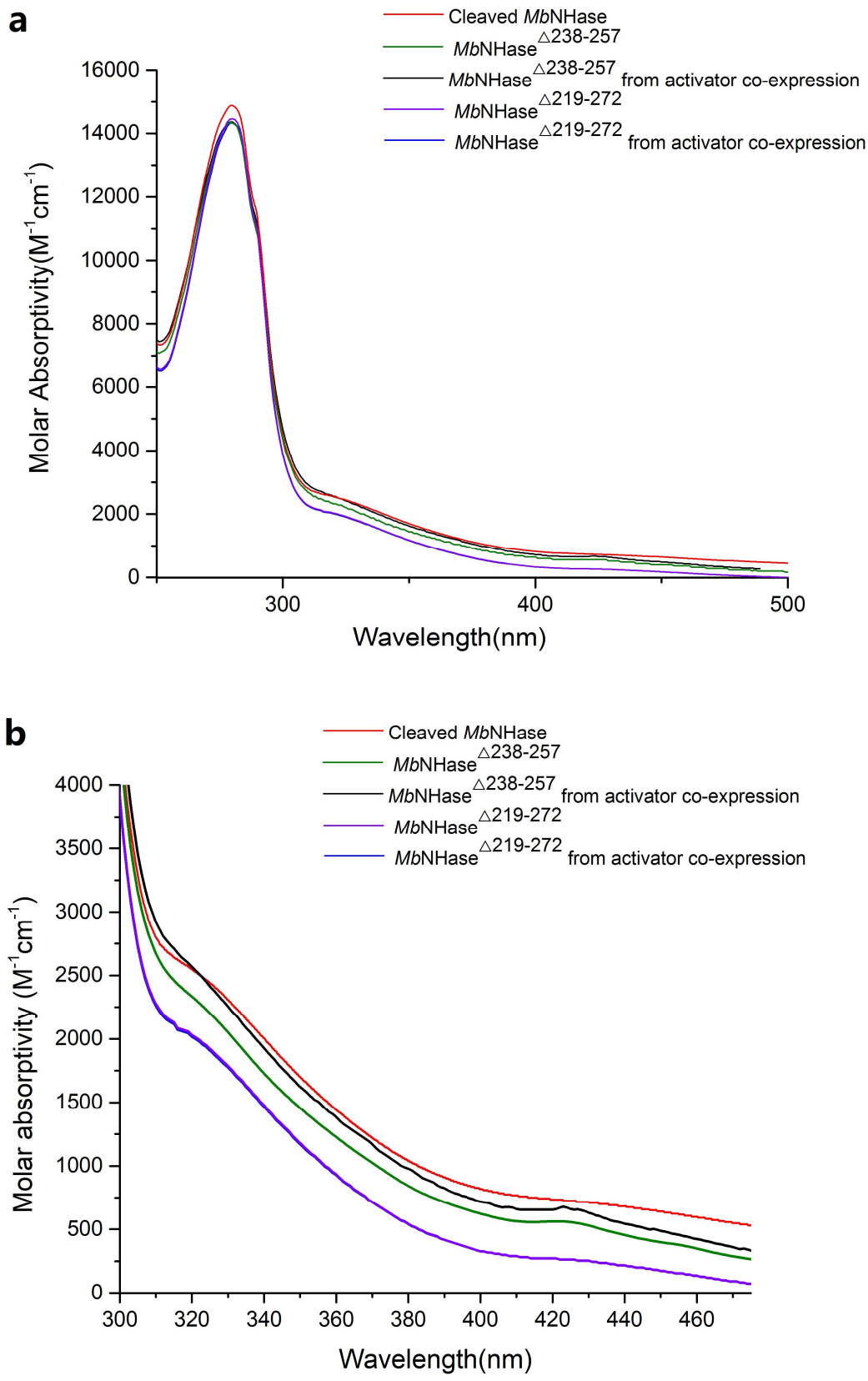
a
Cleaved MbNHase
MbNHase△238-257
MbNHase△238-257 from activator co-expression
MbNHase△219-272
MbNHase△219-272 from activator co-expression
Molar Absorptivity(M-1cm-1)
Wavelength(nm)
b
Cleaved MbNHase
MbNHase△238-257
MbNHase△238-257 from activator co-expression
MbNHase△219-272
MbNHase△219-272 from activator co-expression
Molar absorptivity (M-1cm-1)
Wavelength(nm)

Figure 6

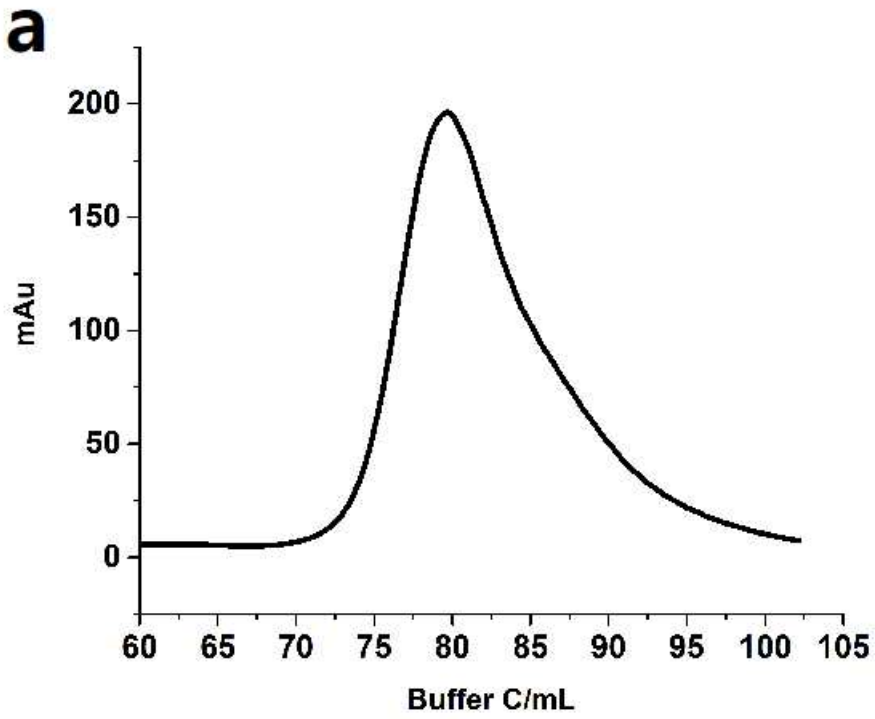
a
200
150
100
50
0
mAu
60
65
70
75
80
85
90
95
100
105
Buffer C/mL

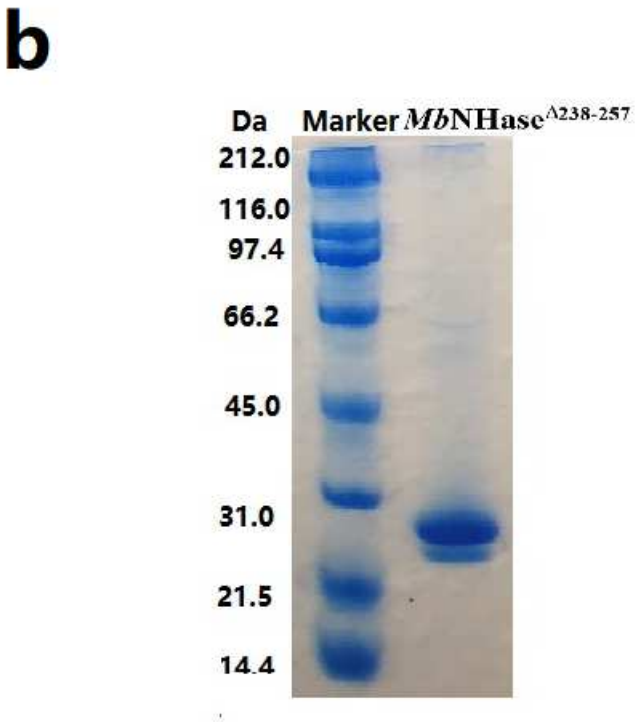
b
Da
Marker
MbNHase^Δ238-257
212.0
116.0
97.4
66.2
45.0
31.0
21.5
14.4

Figure 7

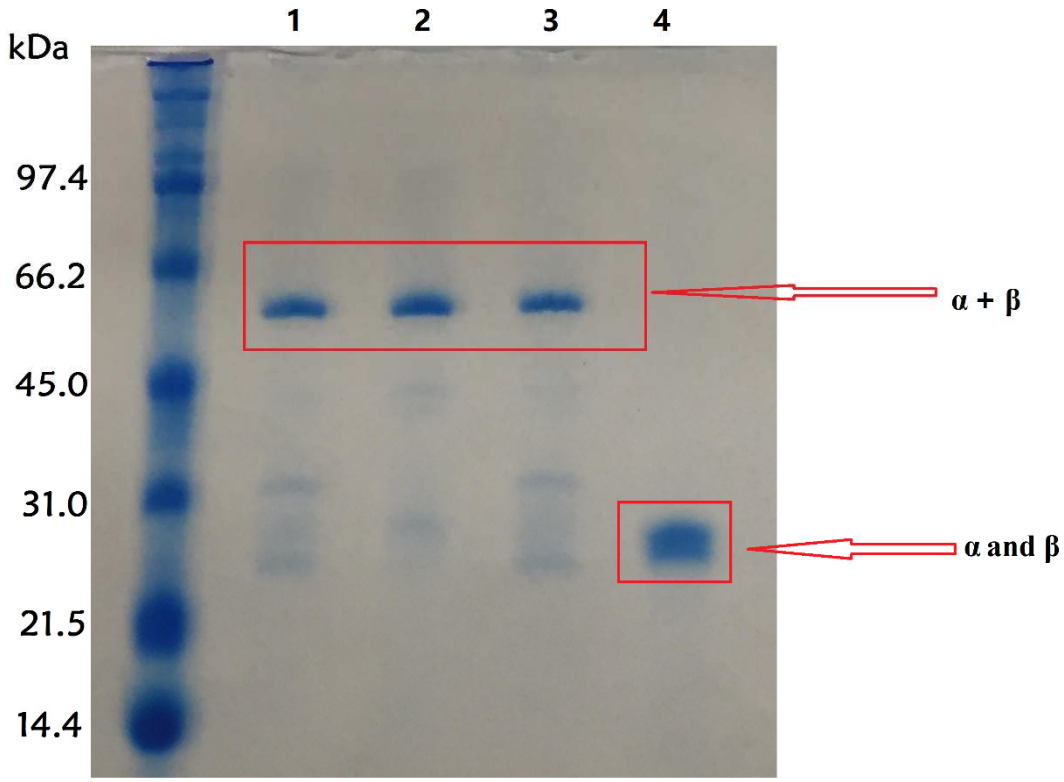

Supplementary Material

Figure SI-1. Gene design for the *Mb*NHase$^{\Delta 238\text{-}257}$ mutant showing that the α and β-subunit genes overlap by sharing the "TG" based on TGA and ATG requiring on one promotor for the expression of both genes.

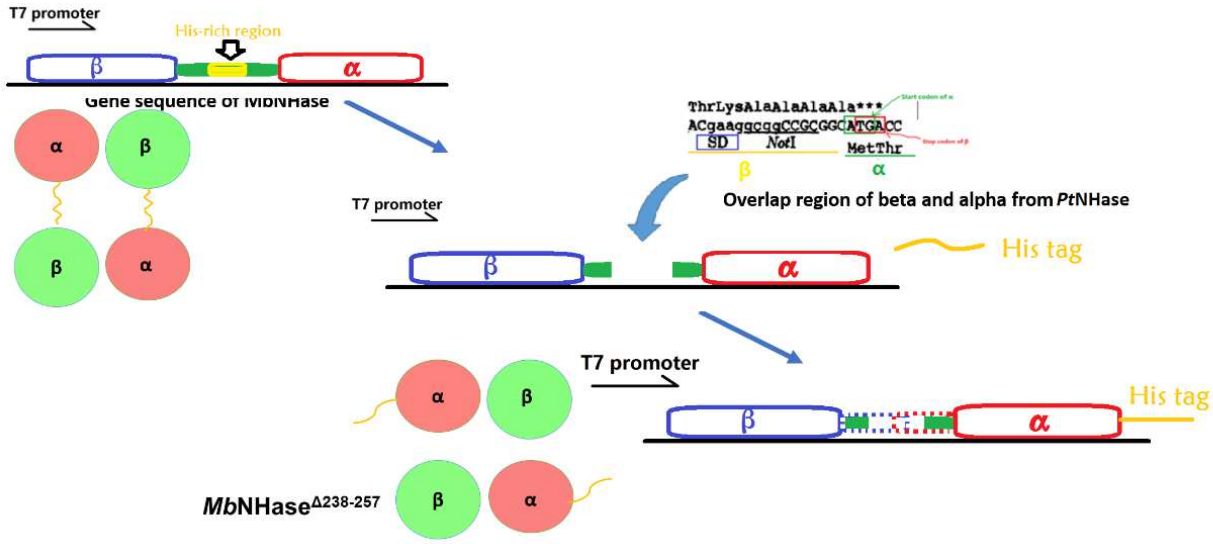

Figure SI-2. EPR spectrum of a 200 µM sample of *Mb*NHase in 50 mM HEPES buffer containing 300 mM NaCl, pH 8.0. Signals observed at g = 4.3 (~1500 G) and g = 2.0 (~3400 G) are Fe(III) and Cu(II) impurities within the EPR cavity.

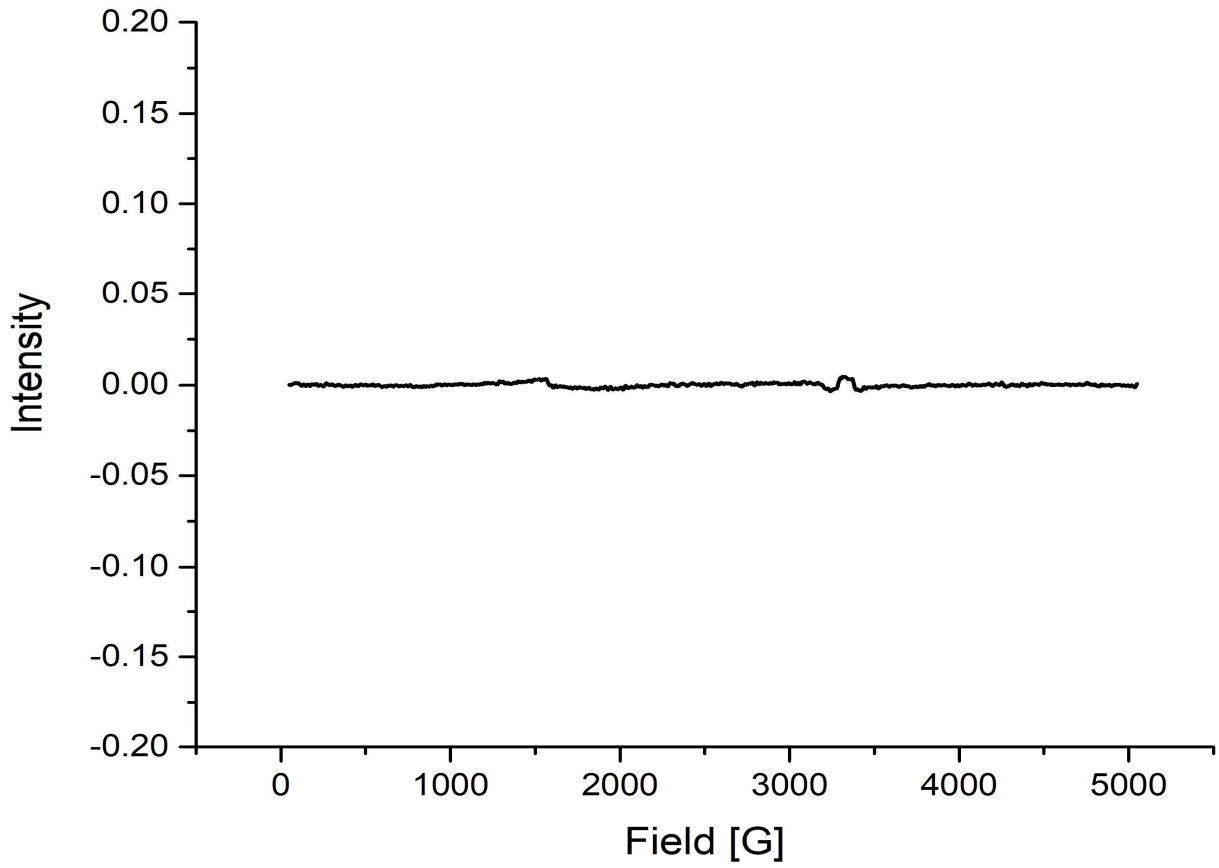

.

Highlights

- Metallocentre assembly in the eukaryotic nitrile hydratase from *Monosiga brevicollis* (*Mb*NHase).
- WT *Mb*NHase expresses as a single polypeptide with fused α- and β-subunits linked by a $(His)_{17}$ and an insert region.
- Two insert region mutant *Mb*NHase enzymes were examined, *Mb*NHase$^{\Delta 238\text{-}257}$ and *Mb*NHase$^{\Delta 219\text{-}272}$.
- Neither the $(His)_{17}$ nor the entire insert region are required for metallocentre assembly and maturation.